

# Molecular and Biochemical Studies of Chondramide Formation—Highly Cytotoxic Natural Products from *Chondromyces crocatus* Cm c5

Shwan Rachid,<sup>1</sup> Daniel Krug,<sup>1</sup> Brigitte Kunze,<sup>2</sup> Irene Kochems,<sup>1</sup> Maren Scharfe,<sup>2</sup> T. Mark Zabriskie,<sup>3</sup> Helmut Blöcker,<sup>2</sup> and Rolf Müller<sup>1,2,\*</sup>

<sup>1</sup>Pharmaceutical Biotechnology

Saarland University

P.O. Box 151150

66041 Saarbrücken

Germany

<sup>2</sup>GBF-German Research Centre Biotechnology

Mascheroderweg 1

38124 Braunschweig

Germany

<sup>3</sup>Department of Pharmaceutical Sciences

Oregon State University

Corvallis, Oregon 97331

## Summary

The jaspamide/chondramide family of depsipeptides are mixed PKS/NRPS natural products isolated from marine sponges and a terrestrial myxobacterium that potentially affect the function of the actin cytoskeleton. As a first step to improve production in heterologous host cells and permit genetic approaches to novel analogs, we have cloned and characterized the chondramide biosynthetic genes from the myxobacterium *Chondromyces crocatus* Cm c5. In addition to the expected PKS and NRPS genes, the cluster encodes a rare tyrosine aminomutase for  $\beta$ -tyrosine formation and a previously unknown tryptophan-2-halogenase. Conditions for gene transfer into *C. crocatus* Cm c5 were developed, and inactivation of several genes corroborated their proposed function and served to define the boundaries of the cluster. Biochemical characterization of the final NRPS adenylation domain confirmed the direct activation of  $\beta$ -tyrosine, and fluorinated chondramides were produced through precursor-directed biosynthesis.

## Introduction

The analysis of natural product formation substantially contributes to our understanding of novel biochemical pathways in vitro and in vivo and consequently makes available not only valuable drugs but also essential tools for biochemistry and molecular cell biology [1, 2]. Approximately two thirds of drugs used to treat cancer or infectious diseases are either natural products or have been developed based on lead structures provided by nature. Among the various sources of compounds for the development of new drugs, microorganisms are of particular significance [3].

Investigations of several species of myxobacteria have resulted in the isolation of a number of interesting secondary metabolites that possess antibiotic and cytotoxic activities [4–6]. Myxobacteria contain a wide

variety of secondary metabolic gene clusters, mostly encoding polyketide synthases (PKSs), nonribosomal peptide synthetases (NRPSs), or PKS/NRPS hybrids [6–8]. Screening fermentations of the myxobacteria *Chondromyces crocatus* Cm c5 for biologically active metabolites resulted in the isolation of a number of exciting secondary metabolites. Strain Cm c5 was found to produce six entirely novel groups of metabolites, including chondramides, crocacin, ajudazole, crocaceptins, thuggacins, and chondrochlorens [9–13]. These metabolites show potent and diverse activities; ajudazols and crocacin A represent inhibitors of the eukaryotic respiratory chain at different sites, while ajudazols inhibit the electron transport at the site of complex I, i.e., NADH:ubiquinone-oxidoreductase [11], crocacin A interferes with the cytochrome *bc1* segment and therefore is highly toxic for mammalian cells, fungi, and yeasts [14, 15]. The extract of *C. crocatus* Cm c5 also yielded a mixture of depsipeptides, the chondramides. Chondramides (A–D) show a high cytostatic activity in mammalian cell cultures (IC<sub>50</sub> 2–60 ng/ml) (Figures 1D and 1E) and are active against some yeasts (MIC 25–50  $\mu$ g/ml) [9]. However, filamentous fungi and bacteria are not inhibited in their growth.

Chondramides are a class of mixed peptide/polyketide depsipeptides comprised of three amino acids (alanine, N-methyltryptophan, plus the unusual amino acid  $\beta$ -tyrosine or  $\alpha$ -methoxy- $\beta$ -tyrosine) and a polyketide chain ([E]-7-hydroxy-2,4,6-trimethyloct-4-enoic acid). These agents are strikingly similar to a family of marine depsipeptides including the prototype jaspamide [16–19], the geodiamolides [20–22], and neosiphoniamolide A [23]. The major difference between the chondramides and jaspamide is a putative acetyl versus lactoyl starter unit for the polyketide moiety, respectively (Figure 2).

Interestingly, about 10% of myxobacterial compounds have been found to interact with the cytoskeleton of eukaryotic cells [4]. While epothilon, produced by *Sorangium cellulosum*, interacts with tubulin [24], rhizopodin and chondramides interfere with the actin system, as does the well-known phalloidin, a toxin from green and white deathcap mushrooms [25, 26]. Chondramides and the marine analogs appear to have the same binding site on actin as phalloidin. In contrast to phalloidin, these depsipeptides penetrate mammalian cells well [13] and allow division of the nuclei but not cell cleavage. The different chondramides have similar activity, with chondramide C having the lowest effective concentration [27].

Fermentation-based methods continue to be the preferred approach for large-scale production of soil and aquatic microbe secondary metabolites [28]. However, many of these organisms grow very slowly [29], and the natural products they produce are often present only in trace amounts. For example, the doubling time of *C. crocatus* Cm c5 is approximately 7 hr at 30°C and the yields of chondramides are only about 4 mg/liter [9], which does not make production in this organism economically feasible. The value of the chondramides and related marine depsipeptides as probes of

\*Correspondence: rom@mx.uni-saarland.de

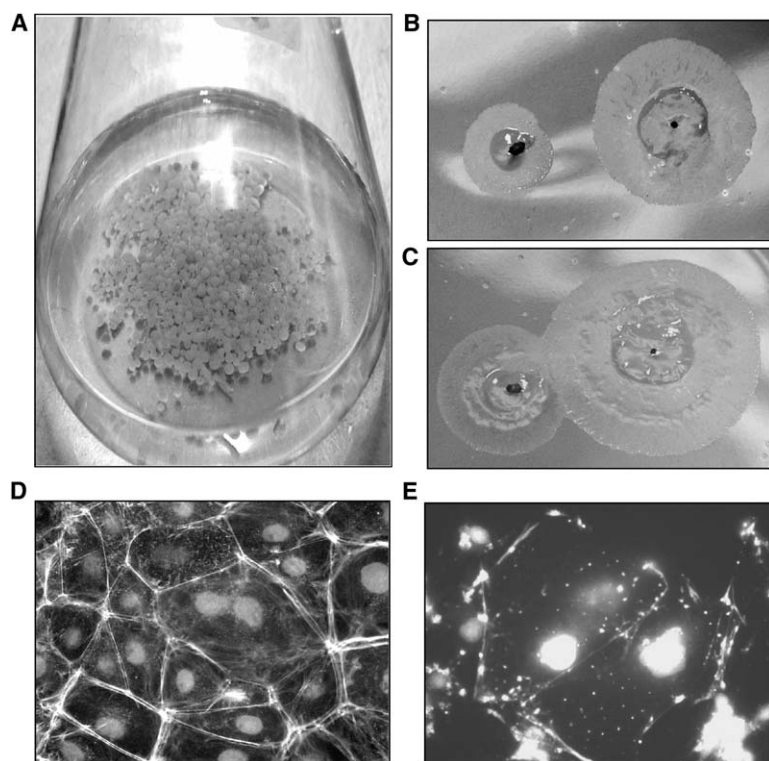


Figure 1. The Growth of *C. crocatus* Cm c5 and the Cytostatic Activity of Chondramides against Cultivated Ptk2 Mammalian Potoroo Cells

(A) Clumps in MD1 medium 7 days after inoculation.

(B and C) Swarming of colonies on Pol03 agar plates (B) after 3 days and (C) after 4 days.

(D) Actin filament and nuclei of the control cells.

(E) Cells after incubation with chondramide show severe shape malformation and reduced number of actin filaments as well as a number of actin knots and clumps. Actin was visualized via staining with Alexa488-phalloidin, and the nuclei were stained with DAPI [13].

actin-mediated cellular functions motivated us to identify the biosynthetic genes encoding their biosynthesis. Furthermore, identification of the biosynthetic genes and elucidation of the biosynthesis pathway is a prerequisite for improving the production through expression of the biosynthetic gene cluster in heterologous host organisms [28, 30, 31]. It is also the essential first step for efforts to increase molecular diversity through combinatorial biosynthesis. Here, we report the cloning of the genes encoding chondramide biosynthesis and the characterization of selected individual gene products. We also describe a method for gene transfer into *C. crocatus*, which was used to inactivate the biosynthetic gene cluster.

## Results

### Identification and Analysis of the Chondramide Biosynthetic Gene Cluster

Based on the chemical structure of the chondramides, we expected a mixed PKS/NRPS pathway also involving a halogenase and a tyrosine aminomutase. To identify the chondramide biosynthetic gene cluster, we employed a screening protocol with probes for PKS and/or NRPS genes. Screening a 2300 clone *C. crocatus* Cm c5 chromosomal library with PKS and NRPS probes identified 40 cosmids that hybridized with both types of probes. Based on the genome size of other myxobacteria [41], this cosmid library represents at least a 10-fold coverage of the genome. Unique hybridizing cosmids were identified by restriction mapping. Cosmid-based PCR amplification of internal NRPS A domain fragments (A3–A10) identified six cosmids that yielded PCR fragments approximately 1200 bp and 2300 bp in size, indi-

ating they carrying typical A domains (1200 bp) and A domain(s) (~2300 bp) harboring an additional domain inserted between these core motifs [34, 42]. Amino acid residues involved in A domain substrate recognition were defined in silico [36, 37] and used in BLAST searches (<http://www.tigr.org/jravel/nrps/blast/index2.html>) of an NRPS substrate specificity database. This analysis revealed that cosmids B:O9, C:K13, and C:O20 all carried A domains predicted to activate glycine, tryptophan, and tyrosine. Moreover, the 2300 bp A domain fragment predicted to activate tryptophan also encodes a N-methyltransferase domain (45.7 kDa in size) inserted between the core motifs A8 and A9. The end sequences of the three cosmid inserts were obtained, and restriction analysis of the cosmids as well as hybridizations with the terminal fragments of each cosmid as probes showed that these three cosmids harbored overlapping sequence. Cosmids C:K13 and B:O9, spanning 49 kb, were sequenced on both strands, and the nucleotide sequence was deposited at EMBO under the accession number AM179409. Sequence analysis revealed that the chondramide (*cmd*) gene cluster was found on a contiguous stretch of 37,807 bp, and the overall GC content of the sequenced region is 68.6%, which is characteristic for myxobacteria [43]. The sequence was analyzed for the presence of putative open-reading frames (orfs) with FramePlot 2.3.2 [44] and preliminary functional assignments of individual orfs was made by comparison of the deduced gene products with proteins of known functions in the database. Thirteen complete orfs were identified, including six likely structural genes for chondramide biosynthesis designated *cmdA*–*cmdF* (Table 1). Apart from orf4 and orf7, all identified genes are transcribed

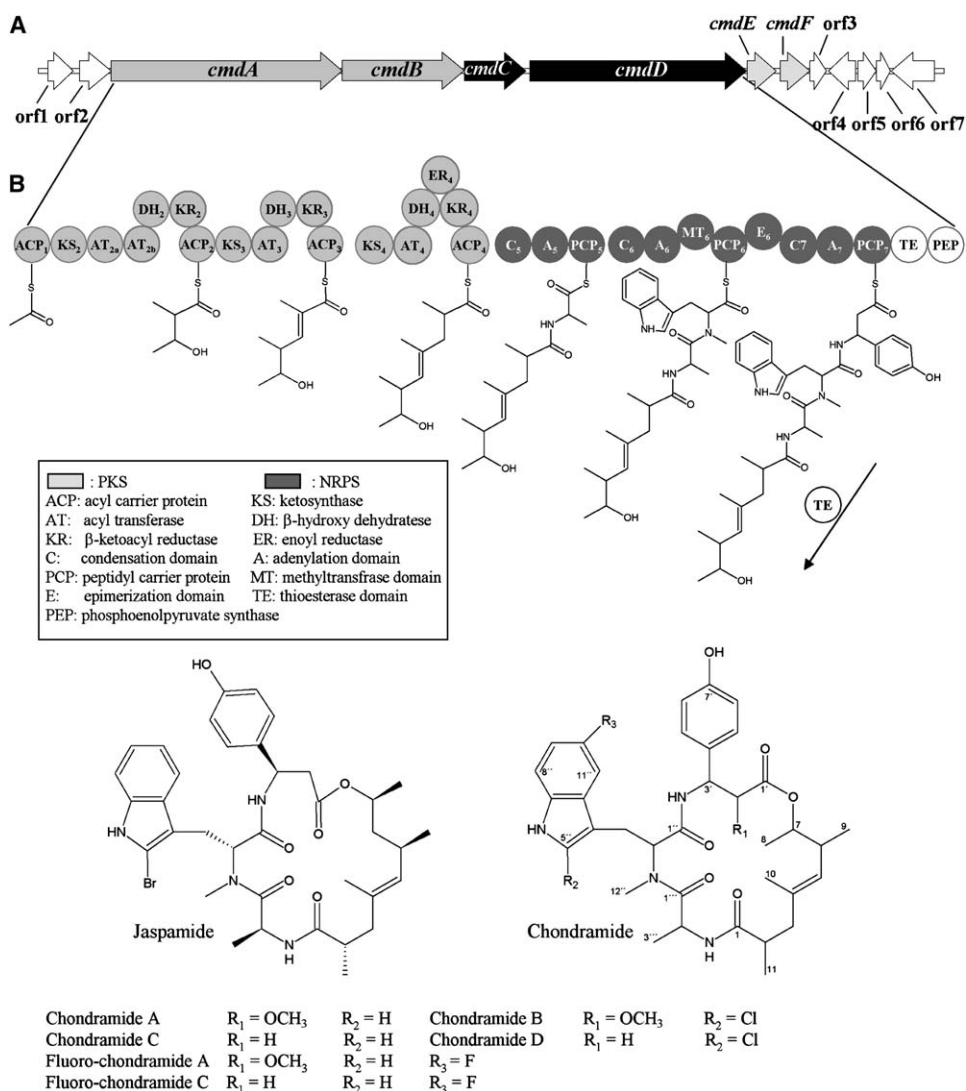


Figure 2. Map and Organization of the Chondramide Biosynthetic Gene Cluster and Model for the Biosynthesis of Chondramide

(A) Map and organization of the chondramide biosynthetic gene cluster.

(B) Model for the biosynthesis of the chondramide skeleton. PKS domains are shown in light gray, and NRPS domains are depicted in dark gray.

in the same direction (Figure 3) and (Table 1). Sequence analysis of the encoded proteins identified typical PKS and NRPS domains located in four orfs (*cmdA*–*cmdD*). The genes *cmdA* and *cmdB* encode for PKSs, while the *cmdC* and *cmdD* encode for NRPSs (Figure 2). According to the results from the inactivation experiments of *orf2* and *orf3*, the chondramide gene cluster begins with *cmdA*, followed by *cmdB* and *cmdC*, which are probably translationally coupled, based on their overlapping stop and start codons (4 bp each), suggesting that they may form part of the same operon. A putative halogenase gene, *cmdE*, is located immediately downstream of *cmdD*. No apparent transcriptional terminator was identified in the intergenic region (52 bp) between *cmdD* and *cmdE*, suggesting they also form an operon. The next gene in the cluster, *cmdF*, encodes a putative tyrosine aminomutase (TAM) and is separated from *cmdE* by an intergenic region that contains an inverted

sequence repeat (*ggcgcgcgtcccgggagcctctccctggacgcgcgcgc*) located 63 bp downstream of the *cmdE* stop codon. This finding indicates the presence of a transcriptional terminator and independent transcription of the downstream genes.

The genes adjacent to the presumed 5' end of the cluster are transcribed in the same orientation and include partial sequence for a putative D-aminoacylase, followed by *orf1* representing a protein with no homology to proteins in the databases and *orf2*, which may encode a phosphoenolpyruvate synthase. The presence of an inverted repeat (*cgtccttcacgacaggaggacg*) in the intergenic region (385 bp) between *orf1* and *orf2* probably terminates transcription from *orf1* and indicates the presence of a putative promoter driving expression of *orf2*. Sequence analysis of the short intergenic region (14 bp) between *orf2* and *cmdA* showed neither a transcriptional terminator nor a promoter sequence in this

Table 1. List of Chondramide Biosynthetic Proteins and orfs Encoded in the Adjacent Genomic Region

Cmd Orfs (A.A.)	Transcriptional Direction and Putative Start Codon/RBS	Proposed Function	Identity/Similarity to Protein/Origin
Orf1 (448)	(+) GTG / GAAG	Unknown	No significant homology
Orf2 (563)	(+) GTG / GGAG	Unknown	31%, 49%: Phosphoenol pyruvate synthase <i>Desulfotobacterium hafniense</i> DCB-2
CmdA (4179)	(+) ATG / GAGG	PKS: ACP <sub>1</sub> KS <sub>2</sub> AT <sub>2a</sub> AT <sub>2b</sub> DH <sub>2</sub> KR <sub>2</sub> ACP <sub>2</sub> KS <sub>3</sub> AT <sub>3</sub> DH <sub>3</sub> KR <sub>3</sub> ACP <sub>3</sub>	38%, 53%: MtaB <i>Stigmatella aurantiaca</i>
CmdB (2198)	(+) GTG / GTGG	PKS: KS <sub>4</sub> AT <sub>4</sub> DH <sub>4</sub> ER <sub>4</sub> KR <sub>4</sub> ACP <sub>4</sub>	58%, 70%: EpoD <i>Polyangium cellululosum</i>
CmdC (1118)	(+) ATG / GTGG	NRPS: C <sub>5</sub> A <sub>5</sub> PCP <sub>5</sub>	42%, 60%: JamO <i>Lyngbya majuscula</i>
CmdD (3912)	(+) ATG / GAAG	NRPS: C <sub>6</sub> , A <sub>6</sub> , MT <sub>6</sub> , PCP <sub>6</sub> , E <sub>6</sub> , C <sub>7</sub> , A <sub>7</sub> , PCP <sub>7</sub> , TE	40%, 57%: NRPS <i>Brevibacillus brevis</i>
CmdE (522)	(+) ATG / GAAG	Halogenase	38%, 55%: putative halogenase <i>Nocardia farcinica</i> IFM 10152
CmdF (531)	(+) GTG / GAAG	Tyrosine aminomutase	45%, 63%: tyrosine amino-mutase <i>Streptomyces globisporus</i>
Orf3 (292)	(+) ATG / GAAG	Unknown	36%, 53%: phosphoenol pyruvate synthase <i>Methanocaldococcus jannaschii</i> DSM 2661
Orf4 (492)	(-) ATG / GGAG	Unknown	41%, 59%: 5'-nucleotidase/2',3'-cyclic phosphodiesterase <i>Anabaena variabilis</i> ATCC 29413
Orf5 (329)	(+) GTG / GGAG	Unknown	26%, 39%: hypothetical protein BpseS_01001321 in <i>Burkholderia pseudomallei</i> S13
Orf6 (253)	(+) ATG / GGAG	Unknown	39%, 52%: cephalosporin hydroxylase <i>Mesorhizobium loti</i>
Orf7 (783)	(-) ATG / GGGG	Unknown	46%, 65%: heavy metal translocating P-type ATPase <i>Methylococcus capsulatus</i> str. Bath

DNA region. Nevertheless, inactivation of orf2 had no effect on chondramide production (data not shown). In silico analysis ([http://www.fruitfly.org/seq\\_tools/promoter.html](http://www.fruitfly.org/seq_tools/promoter.html)) of the DNA region upstream of *cmdA* identified a probable promoter region for the chondramide gene cluster that is located 51 bp upstream of the orf2 stop codon (from nucleotide 1639–1689). The proposed region is not affected by inactivation of orf2 via integration of pSR4.

Orf3 is located downstream of *cmdF* and the translated product shows significant similarity to phosphoenolpyruvate synthases. Inactivation of this gene by insertion of pSR5 into the genome did not change chondramide production (data not shown). Orf4 is oriented in the opposite direction and encodes a protein with high similarities to 5'-nucleotidase and 2',3'-cyclic phosphodiesterase from *Anabaena variabilis*. The product of orf5 shows similarities to a hypothetical protein from *Burkholderia pseudomallei* S13, and orf6 encodes a protein that resembles the cephalosporin hydroxylase of *Mesorhizobium loti* MAFF303099. Inactivation of this gene by insertion of the plasmid pSR6 into the chromosome resulted in no change in chondramide production compared to the wild-type. A short intergenic sequence (12 bp) separates orf6 from orf5; therefore, they are presumed to be transcriptionally coupled. The deduced amino acid sequence of orf7 is markedly similar to the heavy metal translocating P-type ATPase of *Methylococcus capsulatus*. This gene is oriented convergently with the upstream gene, and in the final 612 bp region is a partial sequence (338 bp) of an orf that encodes for a protein with no significant homology to the proteins in the databases.

#### Inactivation of the Chondramide Biosynthetic Gene Cluster

To unambiguously show that the identified region represents the chondramide biosynthetic gene cluster, a method for DNA transfer and gene inactivation was developed for *C. crocatus* Cm c5. This proved to be challenging due to the growth characteristics of the strain and the fast swarming on agar plates (Figures 1B and 1C). Insertion of plasmid pSBO9 carrying an internal fragment of the A<sub>5</sub> occurred by single crossover after DNA transfer by interspecies conjugation with *E. coli* (Figure 3A). The results of Southern blot analysis (Figure 3B) and PCR (data not shown) confirmed the fidelity of the mutation in the chromosome of *C. crocatus* Mut.20. HPLC and HPLC-MS analysis of the mutant extract clearly showed the disappearance of chondramides in the production spectrum in comparison to the wild-type (Figures 3C and 3D).

#### Inactivation of the Halogenase Gene *cmdE*

Sequence analysis suggested *cmdE* encodes a halogenase responsible for formation of the 2-chlorotryptophan residues in chondramides B and D. Integration of the halogenase inactivation plasmid pSHAL into the genome of the *C. crocatus* Cm c5 by single crossover resulted in the inactivation of *cmdE* (Figure 4A). The resulting mutant Cmc-Hal<sup>-</sup> was confirmed by PCR analysis, which generated a fragment of 1223 bp in the mutant and no fragment in the wild-type (data not shown). To determine if the inactivation of *cmdE* leads to a polar effect influencing the expression of the downstream gene, *cmdF*, Northern blot analysis of total RNA in the *cmdE* mutant was performed. The results indicate that



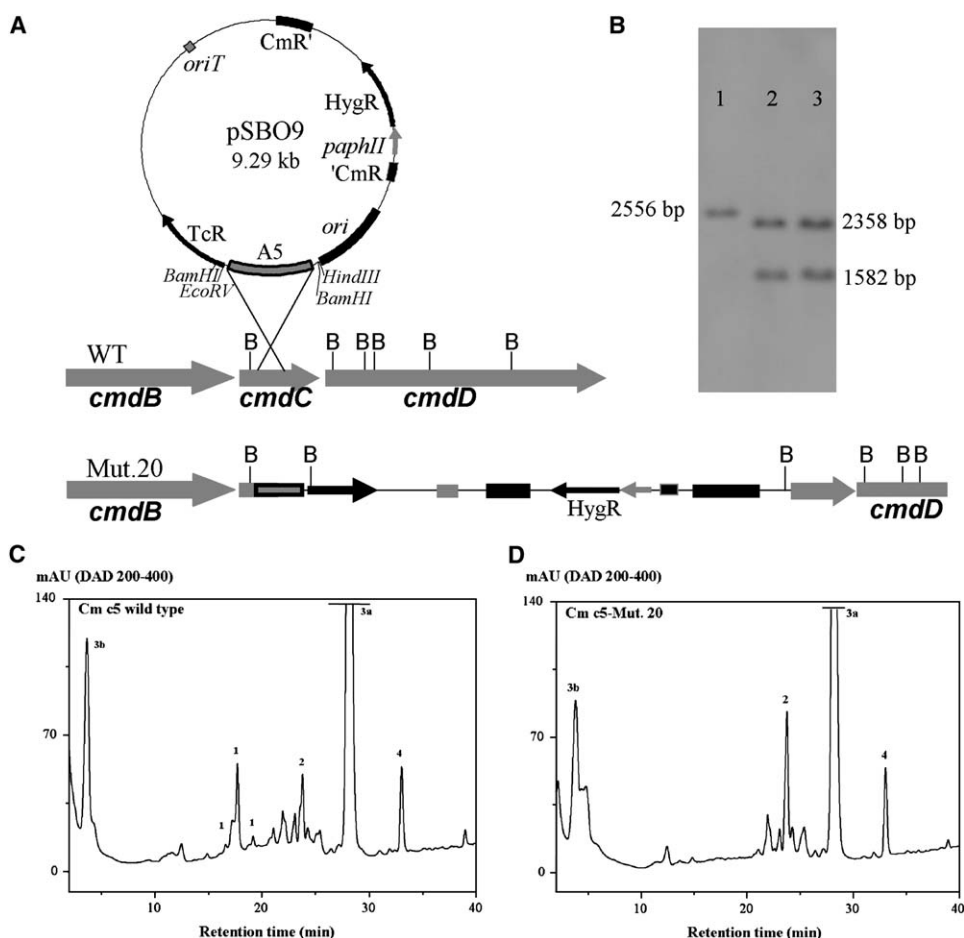


Figure 3. Inactivation of the Chondramide Biosynthetic Gene Cluster by Single Crossover Homologous Recombination Using the pSB09 Inactivation Plasmid

(A) Schematic representation of pSB09 and the organization of the resulting mutant chromosome.

(B) Southern blot analysis of the *C. crocatus* Cm c5 (lane 1) and the Mut.20 chromosome (lanes 2 and 3) digested with *Bam*HI and hybridized with a DIG-labeled internal fragment of the module 5 adenylation domain from the chondramide gene cluster.

(C) HPLC analysis of the wild-type *C. crocatus* Cm c5 methanolic extract.

(D) Methanolic extract of *C. crocatus* Mut.20. Peaks corresponding to chondramides (1), chondrochloren (2), crocacin A (3a), and crocacin B (3b) and ajudazol (4) are indicated.

transcription of *cmdF* is reduced in the mutant but not abolished (Figure 4B). Subsequent HPLC-MS analysis of the *cmdE* mutant culture showed that instead of the normal chondramide mixture, only the nonchlorinated chondramides A and C were present. However, the production was 10-fold lower in the mutant compared to the wild-type (Figures 4C and 4D).

#### Incorporation of 5-Fluorotryptophan into Chondramides

An experiment to incorporate tryptophan analogs into the chondramides was performed. Addition of 5-fluorotryptophan to cultures of *C. crocatus* Cm c5, followed by HPLC-MS/MS analysis, revealed the presence of new peaks (Figure 5). The new compounds were shown to correspond to fluoro-chondramide A (rt = 17.4 min; MW 665.4; [M+H]<sup>+</sup>) and fluoro-chondramide C (rt = 18.4 min; MW 635.4 [M+H]<sup>+</sup> and 657.3 [M+Na]<sup>+</sup>). However, fluorinated analogs of chondramides B and D were not found in the extract.

#### Cloning, Expression, and Characterization of the A<sub>7</sub> Domain

Heterologous expression of the GST-tagged A<sub>7</sub> domain, approximately 89 kDa in size, was achieved by using pGEX-Ad-7 in *E. coli* BL21. The fusion protein was found in the soluble fraction after French press lysis of *E. coli* cells, as judged by Coomassie blue-stained SDS-PAGE. Purification by GST affinity column chromatography and digestion with PreScission protease yielded the purified A domain (62 kDa in size) (Figure 6B). The substrate specificity of the A domain was investigated by the ATP-PPi-exchange reaction [40]. Incubation with various amino acids, including (*R,S*)-β-tyrosine, in the presence of [<sup>32</sup>P]-pyrophosphate revealed the highest activity with β-tyrosine (normalized to 100%; negative controls without enzyme gave 0.1%–1% of this activity). This result corresponds well with the position of A<sub>7</sub> within the CmdD protein (Figure 2B). L-tyrosine was found to be activated equally well (95%) as β-tyrosine and L-phenylalanine was activated to a lesser extent

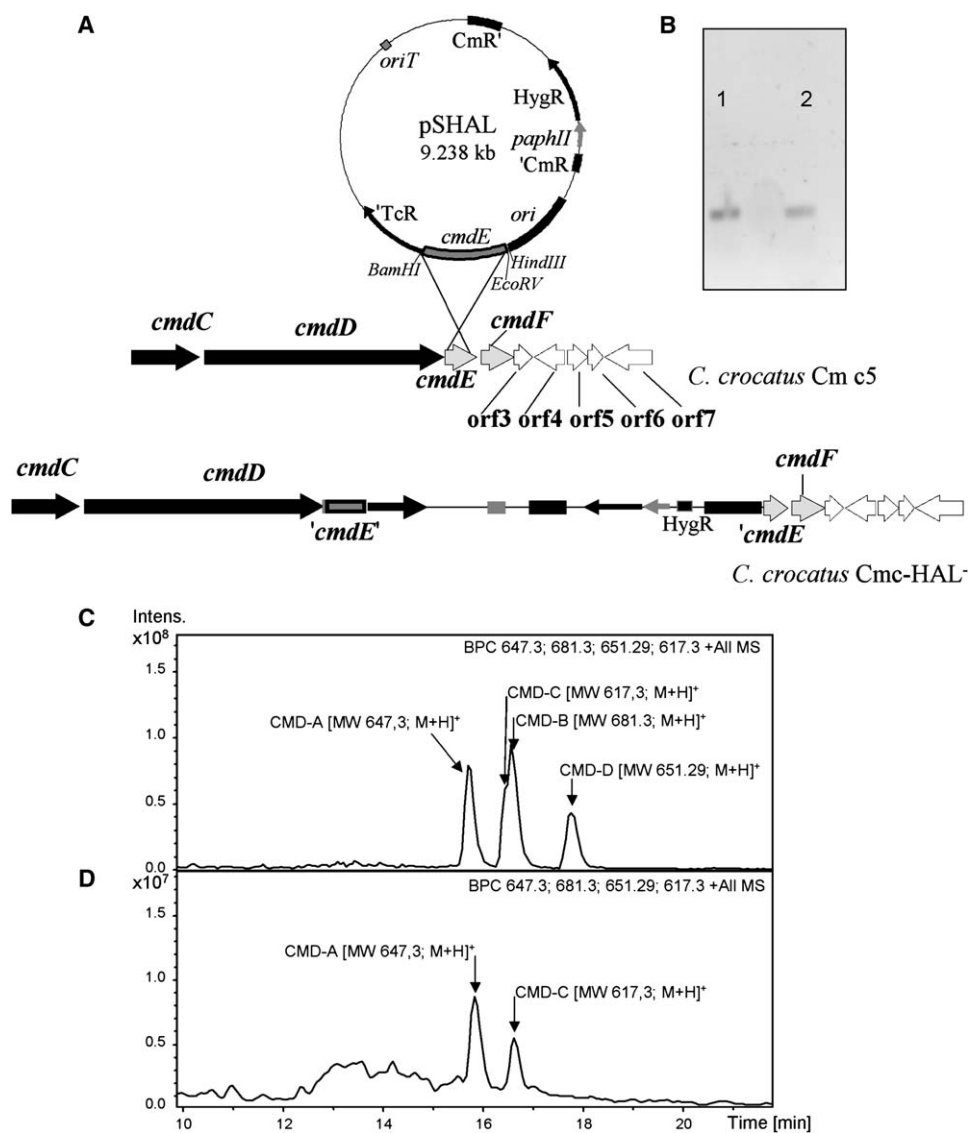


**Figure 4.** Inactivation of the *cmdE* Gene by Single Crossover Homologous Recombination Using the pSHAL Inactivation Plasmid  
(A) Schematic representation of pSHAL and the organization of the resulting mutant chromosome.  
(B) Northern blot analysis of total RNA from *C. crocatus* Cm c5 (lane 1) and *C. crocatus* Cmc-Hal<sup>-</sup> (lane 2) hybridized with a DIG-labeled internal fragment of the *cmdF* gene.  
(C) HPLC-MS analysis of *C. crocatus* Cm c5 methanolic extract.  
(D) Identical analysis of *C. crocatus* Cmc-Hal<sup>-</sup> showing the disappearance of both halogenated chondramides (B and D).

(30%). Both tryptophan and methionine gave rise to background-level activity (Figure 6A).

## Discussion

Chondramides A–D are depsipeptide antitumor and antifungal antibiotics produced by *C. crocatus* Cm c5, differing structurally in modifications to the tryptophan and  $\beta$ -tyrosine residues (Figure 2B). We set out to clone the *cmd* biosynthetic gene cluster to better understand the formation of these hybrid polyketide–peptide natural products in myxobacteria and to subsequently help facilitate the cloning of their marine counterparts, like jaspamide. For this purpose, a *C. crocatus* Cm c5 gene library was constructed and screened by colony

hybridization with general NRPS and PKS probes amplified by PCR [8, 34]. Initially, we did not expect to be able to perform chromosomal mutagenesis in *C. crocatus* Cm c5 (see below) and therefore chose an alternative approach to screen for the biosynthetic genes (see Experimental Procedures). A gene cluster containing PKS and NRPS genes consistent in sequence and architecture with that predicted to assemble the chondramide structure was identified on two overlapping cosmids, B:O9 and C:K13. While most *C. crocatus* strains only grow in the presence of a companion bacterium, and thus have to be fermented as mixed cultures [45], *C. crocatus* Cm c5 can grow in a pure culture. However, the strain grows in the form of clumps and flakes (Figure 1A), and no homogeneous cell suspensions are obtained.

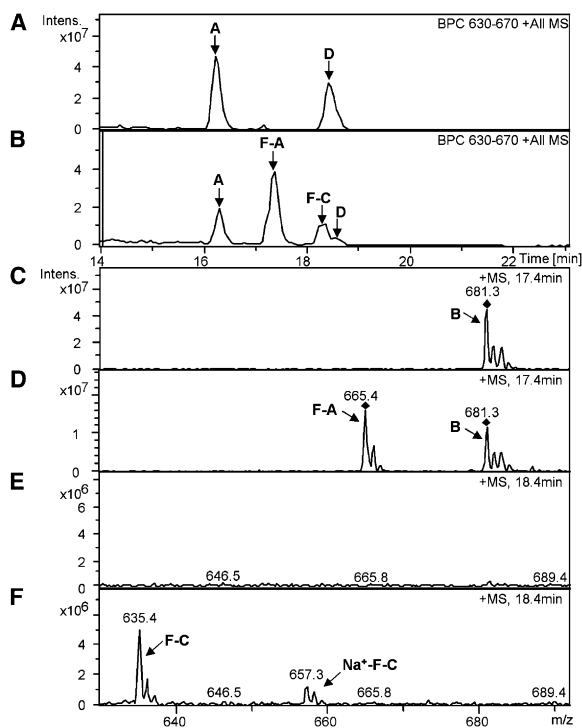


Figure 5. HPLC-MS Analysis of the Production of Fluorochondramide Analogs

HPLC-MS analysis of chondramide production in *C. crocatus* Cm c5 after growth in Pol0.3 medium (A) and in Pol0.3 supplemented with 1 mM 5-fluorotryptophan (B). A, chondramide A; F-A, fluorochondramide A; B, chondramide B; C, chondramide C; F-C, fluorochondramide C; Na<sup>+</sup>-F-C, sodium peak of fluorochondramide C; and D, chondramide D. (D) The mass spectra of (B) at 17.4 min shows F-A (MW 665.4; M+H)<sup>+</sup> and chondramide B [MW 681.3; M+H]<sup>+</sup>, and the same analysis with sample (A) is given in (C). (F) The mass spectra of (B) at 18.4 min shows F-C (MW 635.4; M+H)<sup>+</sup> and Na<sup>+</sup>-F-C (MW 657.3; M+Na)<sup>+</sup>, and the same analysis with sample (A) is given in (E).

Normal plating of the strain does not yield single cell colonies, and the mixed colonies develop only very slowly (7–10 days). Furthermore, selection of a single genotype after plating on an agar surface is problematic. This is due to sudden and fast swarming of the bacteria toward neighbor clones (Figures 1B and 1C). In addition, the bacteria exhibit resistance against almost all antibiotics

tested (e.g., ampicillin, kanamycin, streptomycin, apramycin, tetracycline, spectinomycin, gentamicin, and tobramycin). Only hygromycin was found to be useful as a selection marker for the genetic work. Fortunately, we were able to develop a gene inactivation strategy for *C. crocatus* Cm c5. Inactivation of the NRPS gene *cmdC* in the cloned gene cluster via homologous recombination abolished chondramide production in the resulting mutant *C. crocatus* Mut.20 (Figure 3). The deduced function of the proteins encoded on cosmids B:09 and C:K13 (Table 1) are also consistent with their involvement in chondramide biosynthesis.

### A Proposed Biosynthetic Pathway to Chondramides

The chemical structure of chondramides suggests type I PKSs and NRPSs are involved in their biosynthesis. These multifunctional enzymes catalyze the formation of polyketides by condensation of simple carboxylic acids and of peptides via the assembly of amino acids. The molecular logic of PKS and NRPS systems has generally been interpreted in light of known product structures. By using the predicted substrate specificity of individual NRPS [34, 37] and PKS modules [46–48] as a guide, the PKS and NRPS modules encoded in the *cmd* gene cluster can be aligned to constitute the chondramide megasynthetase shown in Figure 2. The biosynthetic system of chondramides shows a high level of colinearity between genes in the cluster and the predicted biochemical steps required for chondramide biosynthesis, which is not always the case in myxobacterial biosynthetic systems [49–53].

Analysis of the modular structure of CmdA revealed that it most likely encodes the initial three modules of the megasynthetase. Similar to several myxobacterial PKSs, CmdA shows an atypically arranged starter module plus one extension module ACP<sub>1</sub>-KS<sub>2</sub>-AT<sub>2a</sub>-AT<sub>2b</sub>-DH<sub>2</sub>-KR<sub>2</sub>-ACP<sub>2</sub>-KS<sub>3</sub>-AT<sub>3</sub>-DH<sub>3</sub>-KR<sub>3</sub>-ACP<sub>3</sub> [33, 49, 54–56]. In these systems, the first AT loads the starter molecule, whereas the second AT is responsible for the first extending unit [56, 57]. The initiation step of chondramide biosynthesis includes selection and loading of the starter unit acetyl-CoA to ACP<sub>1</sub> and loading of ACP<sub>2</sub> with methylmalonyl-CoA (mmCoA). All AT domains of the *cmd* gene cluster contain the conserved active site motif GHSXG. The computational approach to identify AT<sub>2b</sub>, AT<sub>3</sub>, and AT<sub>4</sub> substrate specificity relied on identification of 13 key residues that can be compared to AT

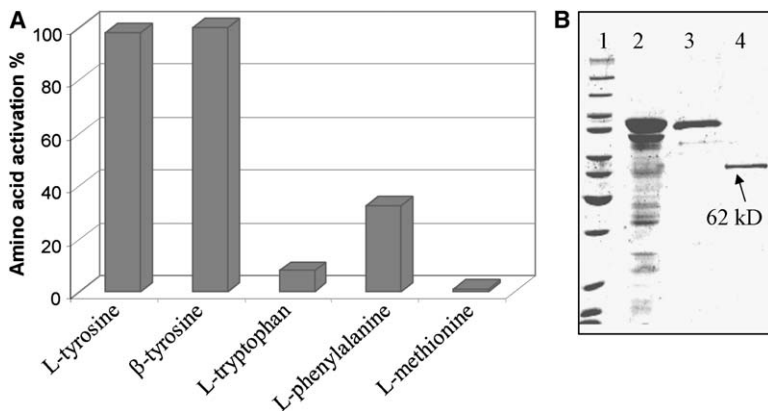


Figure 6. Analysis of Recombinant Module 7 Adenylation Domain, A<sub>7</sub>

(A) ATP-PPi exchange assay. The diagram shows the relative activity compared to β-tyrosine, normalized to 100%. (B) Overexpression and purification of the A<sub>7</sub> protein. Lane 1, MW markers; lane 2, extract of IPTG-induced *E. coli* BI21-pGEX-Ad<sub>7</sub> cells; lane 3, GST-tagged A<sub>7</sub> protein (~89 kDa) after GST-affinity chromatography; and lane 4, purified A<sub>7</sub> after digestion with PreScission protease.

## A

	11	63	90	91	92	93	94	117	200	201	231	250	255	15	38	59	60	61	62	70	72	197	198	199
AT <sub>2a</sub>	Q	F	G	H	S	T	G	Q	P	H	E	N	A	W	H	I	E	V	S	D	A	N	V	A
AT <sub>2b</sub>	Q	Q	G	H	S	M	G	R	S	H	T	N	V	W	E	I	D	V	V	E	A	D	V	A
AT <sub>3</sub>	Q	Q	G	H	S	M	G	R	S	H	T	N	V	W	R	I	D	V	V	E	A	D	V	A
AT <sub>4</sub>	Q	Q	G	H	S	M	G	R	S	H	T	N	V	W	R	I	D	V	V	E	A	D	V	A

## B

```

DH3  AGGHPLLGEALSVSTLSGLRVWETTLDLGRLPWLRDHRVQDLVVFPGAGYLEMALCAGRT 60
DH4  AGEHPLLGEGLSVSASAGMHLWETTLDHDLRPLWLQDHRVQGLLVFPGAGYLEMALSAGRS 60
DH2  SGQHPLLGAPFTSSRHPGEQFWQNDVSRRVPWLSDHRIGDEILPGSATLEMVLAAGAS 60
      :*  *****  ::  *  . *  . : * : .  .  * : *****  * : .  : : * : .  * * * . * : * :
DH3  LWGERPFAVTDVALVEALTLTDEDETPVQLVTTTPQADGNVQMVASRRGAGQDGDWTVHA 120
DH4  LWGEHPLAVTDVALIEALTPADDEPTVQMVTSTQGEALARFQIASQRPAATSAGWTVHA 120
DH2  LYGSSGFETISELRLEKMLSLP----CAILELSIVRSDAGAAAVEIASR--ARAAVAWERYG 114
      * : * .  : : : : * : * : .  .  : : : : * : .  . : * : * : * : * : * : * : * :
DH3  RGTGLGLVAPAEAPAR-VDLGAVRARLRKVLSEGAIHALLSEMGLVYGPAFRGL 172
DH4  RGMRLRLDHASAPDR-VDLGALRARFDQVLAGEEIIYRLLSARGLDYGPFRGL 172
DH3  RAELRQVRGEEQTSAGETLSRIQERCRRELDVAEHHARLERLGIYGPRLQSV 167
      * . * :  . . . * . : : * : * :  : * . * : * * * : : :

```

sequences of known substrate specificity and showed a distinct pattern (QQGHSMGRSHTNSV) (see Figure 7A) similar to the characteristic motif of mmCoA specific AT domains [47, 58]. However, the residues involved in substrate specificity of AT<sub>2a</sub> differ significantly from those found in AT<sub>2b</sub>, AT<sub>3</sub>, and AT<sub>4</sub> (Figure 7A). The conserved motif of AT<sub>2a</sub> is more typical of that for the activation of benzoate (as observed in the soraphen synthase), but it might be substrate limited in vivo in the chondramide producer. Several other ATs have been described that do not fit into the consensus sequences published [58, 59]. According to these data, we propose that the first AT domain in module 2 of the chondramide PKS recognizes the starter unit, acetyl-CoA, and covalently attaches it to ACP<sub>1</sub>. This is followed by transacylation to the KS<sub>2</sub> domain of the first elongating module. The other AT domain, AT<sub>2b</sub>, recognizes mmCoA and loads it onto the second ACP [54, 57]. Both the second and the third PKS modules contain auxiliary DH and, KR domains, which should theoretically catalyze the formation of double bond intermediates. The typical active site (LxxHxxxGxxxxP) of DH domains [60] and the motif for NADP(H) binding (GxGxxAxxxA) [61] essential for KR domains are found in both modules. However, comparison of the DH<sub>2</sub> sequence to functional dehydratases shows low homology and the presence of two sequence gaps (Figure 7B). Because a functional DH<sub>2</sub> is not in accordance with the final structure (the hydroxyl group found at C7 is essential for the thioesterase catalyzed cyclization), the DH in module 2 seems to be inactive. A conserved LDD motif and residues P144 and N148 of the KR<sub>3</sub> domain are characteristic of B-type ketoreductases [62] and correlate well with *trans* configuration of the C4-C5 double bond [10].

The PKS CmdB harbors one module possessing a complete reductive loop (KS, AT, DH, ER, KR, and ACP). This module is involved in another extension with mmCoA and perfectly matches the last step of

Figure 7. Comparison of the PKS AT Domains and Alignment of the Chondramide Synthase DH Domains

(A) Comparison of the PKS AT domains (AT<sub>2a</sub>, AT<sub>2b</sub>, AT<sub>3</sub>, AT<sub>4</sub>) of chondramide synthase. The residue number in the first row corresponds to the position in the *E. coli* fatty acid acyltransferase crystal structure [48, 92]. Identical residues are shaded in gray.

(B) Alignment of the chondramide synthase DH domains depicting conserved histidine and proline residues in bold. The alignment also shows the amino acid sequence of DH<sub>2</sub>, and gray indicates amino acids that are different from the corresponding amino acids in both DH<sub>3</sub> and DH<sub>4</sub>.

PKS chain biosynthesis. At this stage, the CmdB tethered polyketide intermediate is transferred to the PCP bound alanine by the C domain of CmdC. The CmdC NRPS represents a minimal elongation module (C<sub>5</sub>-A<sub>5</sub>-PCP<sub>5</sub>). The substrate specificity of NRPS A domains is determined by the amino acid binding pocket, consisting of a stretch of approximately 100 amino acid residues found between the highly conserved motifs A4 and A5 [63]. Eight specific residues in this region determine the nonribosomal code, which is widely used for substrate prediction [34, 37]. The deduced substrate code for the CmdC A domain (DLFNNALT) is identical to that of McyA of the microcystin gene cluster in the cyanobacterium *Anabaena* strain 90 [64] and also to that of JamO of the jamaicamide biosynthesis gene cluster in *Lyngbya majuscula* [65]. Both of these enzymes are predicted to incorporate alanine based on the structures of the respective peptide products. In the chondramide biosynthesis, an alanine unit is also incorporated at this point.

The next protein of the assembly line, CmdD, harbors NRPS module 6 (C<sub>6</sub>-A<sub>6</sub>-MT<sub>6</sub>-PCP<sub>6</sub>-E<sub>6</sub>) and 7 (C<sub>7</sub>-A<sub>7</sub>-PCP<sub>7</sub>), which nicely explain the final steps in chondramide biosynthesis in agreement with the colinearity rule [34]. Sequence analysis of the A<sub>6</sub> substrate binding pocket (DGVQMAGV) shows 62% identity to the specificity pocket of the TycB3 A domain in *Bacillus brevis*. TycB3 is involved in selection and activation of L-tryptophan, which has been confirmed experimentally [66]. A methyltransferase (MT<sub>6</sub>) domain is found inserted between the core motifs A8 and A9 of A<sub>6</sub>. The positioning of this domain supports its role in catalyzing *N*-methylation of the tryptophan residue. The amino acid sequence of MT<sub>6</sub> carries three of the conserved core motifs for S-adenosyl methionine-dependent MTs: LEIGTGTG, GFSAGQFDTIV, and LKPGGTLFL [67]. The incorporation of D amino acids into secondary metabolites is a special feature occurring in nonribosomal peptides.



In rare instances, D amino acids can be provided by external racemases recognized by a specific A domain [68]. More commonly, epimerization (E) domains are integrated into a module and catalyze the inversion of PCP bound L amino acids (in initiation modules) or L-peptidyl moieties (in elongation modules) [68–70]. Subsequently, only the D-aminoacyl or D-peptidyl-ender is selected by the downstream C domain for condensation with the next building block [71, 72]. The E<sub>6</sub> domain found downstream the PCP<sub>6</sub> of the chondramide gene cluster is predicted to epimerize tryptophan loaded by the NRPS module 6. After epimerization, the C<sub>7</sub> domain discriminates against the L isomer, and only the D isomer is incorporated into the product. E domains share a conserved HHXXDG motif and the second histidine residue seems to be directly involved in catalysis [69, 73]. Although the stereochemistry of the tryptophan residue in the chondramides is unknown, the E<sub>6</sub> domain carries the corresponding conserved residues (HHLVVDG), which argues for its catalytic activity.

The last NRPS module in CmdD is a termination module (C<sub>7</sub>-A<sub>7</sub>-PCP<sub>7</sub>-TE) that includes a thioesterase (TE) domain. The substrate specificity code for module 7 (DGSTITAV) shows 75% identity with tyrosine incorporating modules in two cyanobacterial systems: AdpB, involved in anabaenopeptilide biosynthesis [74], and NosD1, required for nostozeptolide A biosynthesis [75]. However, chondramide assembly requires the incorporation of the unusual amino acid  $\beta$ -tyrosine by the terminal NRPS module. Naturally occurring  $\beta$  amino acids are relatively rare, and in almost all cases, the  $\beta$  amino acids are formed by an intramolecular migration of the  $\alpha$ -amino group. A number of aminomutases catalyzing these reactions have been characterized and include several involved in secondary metabolism [76–78]. A putative tyrosine aminomutase (TAM) gene is located downstream of *cmdE*, and the translated product shows high similarity to the TAM that functions in C-1027 biosynthesis in *Streptomyces globisporus* [78]. This similarity includes the signature Ala-Ser-Gly motif common to the family of ammonium lyases. The TAM from *S. globisporus* (SgcC4) has been intensively studied and shown to possess ammonium lyase and aminomutase activity through elimination and subsequent Michael addition of ammonium to the  $\alpha$ - $\beta$  unsaturated acid prior to its release [78]. It was further demonstrated that the enzyme utilizes a 4-methylideneimidazole-5-one (MIO) as cofactor, which is formed autocatalytically from the conserved ASG sequence motif. Interestingly, SgcC4 preferentially catalyzes the formation of (S)- $\beta$ -tyrosine [78–80], but (R)- $\beta$ -tyrosine is found in jaspamide [16]. Although the absolute stereochemistry of chondramides has not been independently solved, the NRPS domain organization suggests that at least the alanine and tryptophan residues should possess the same configuration as jaspamide.

As described above, a specificity code for A domains has been developed [36, 37, 81]. However, numerous deviations from this “nonribosomal code” have been described [50], and only studies using purified enzyme provide a detailed insight into substrate specificity. Because of the similarity of the A<sub>7</sub> binding pocket to tyrosine activating domains, and due to the fact that no studies have been performed on  $\beta$  amino acid acti-

vating NRPS domains, we set out to characterize this domain biochemically. The A<sub>7</sub> gene fragment was cloned and heterologously expressed in *E. coli* BL21. After purification, the specificity of the enzyme was examined by the standard amino acid-dependent ATP-PPi exchange assay [40]. Of the five amino acids tested, A<sub>7</sub> showed equal activity when presented with (R,S)- $\beta$ -tyrosine or L- $\alpha$ -tyrosine (see Figure 6A). However, because racemic  $\beta$ -tyrosine was used, each enantiomer was present at 1 mM rather than the 2 mM concentration of L-tyrosine. While the question remains whether A<sub>7</sub> in vivo also activates both tyrosine and  $\beta$ -tyrosine, the findings in vitro suggest  $\beta$ -tyrosine is the preferred substrate. In addition, the “wrong” enantiomer present in the assay performed might inhibit the activation reaction. Presumably, in vivo PCP<sub>7</sub> and the TE domain perform some gatekeeper function similar to that described for C and TE domains [71, 82] and discriminate against activated tyrosine since  $\beta$ -tyrosine is the only extender unit found in the known chondramides. The stereochemistry of chondramide and the stereospecificity of TAM and A<sub>7</sub> need to be addressed in future work. Finally, once the elongated chain reaches the final PCP domain, cyclization and release of the completed PKS/NRPS hybrid structure is catalyzed by the TE domain [83].

The biosynthesis of chondramides B and D requires the action of a specific halogenase and CmdE shows significant similarity (55%) and identity (35%, each given on protein level) to other FADH<sub>2</sub>-dependent halogenases. It has been determined that FADH<sub>2</sub> is produced by nonspecific flavin reductases that are required by these halogenases [84]. The chondramide halogenase, CmdE, represents a rare tryptophan 2-halogenase. Free 2-chlorotryptophan is unstable and degrades rapidly under various conditions (U. Kazmaier, personal communication). Due to the natural occurrence of chondramides A and C, it is likely that CmdE modifies an NRPS bound species or the nascent product of the NRPS. Additionally, subsequent chlorination avoids the risk of halogenating free tryptophan required for protein synthesis. Moreover, CmdE shows only 20% identity with the regioselective tryptophan 5-halogenase (PyrH) involved in pyrroindomycin biosynthesis in *Streptomyces rugosporus* LL-42D005 [85] and homology to only the FAD binding domain at the N terminus of the tryptophan 7-halogenase (PrnA) from *Pseudomonas fluorescens* [84]. CmdE exhibits no significant similarity to RebH of the *Lechevalieria aerocolonigenes*, which is involved in generating 7-chlorotryptophan during the biosynthesis of rebeccamycin [86]. To prove the function of CmdE in chondramide biosynthesis, an inactivation of the chondramide halogenase in *C. crocatus* Cm c5 was carried out (Figure 4A). The resulting mutant only produced the nonchlorinated metabolites, chondramides A and C (Figures 4C and 4D). Interestingly, when 5-fluorotryptophan was fed to cultures of *C. crocatus* Cm c5, subsequent HPLC-MS analysis showed that in addition to chondramides (A–D), fluorinated analogs of chondramides A and C were produced (Figure 5). However, fluorochondramide B and fluorochondramide D, which would have 2-chloro-5-fluorotryptophan residues, were not detected. This finding indicates that the megasynthetase does not discriminate against 5-fluorotryptophan as extender unit, but the fluorine most likely

deactivates the indole such that it cannot attack the activated chlorine species (probably HOCl) [84]. Alternatively, the fluorine may affect the hydrogen bonding ability of the indole so that it is not properly positioned in the CmdE active site.

On first inspection, the *cmdF*-encoded TAM seems to be transcriptionally coupled to *cmdE* and essential for chondramide biosynthesis (see above). Nevertheless, *cmdF* is expressed independently from the upstream genes of the gene cluster since its transcription is reduced but not abolished in the *cmdE* minus background (Figure 4B). This finding and the presence of a putative terminator sequence 20 bp downstream of the *cmdE* gene suggests the presence of a promoter region in the intergenic gap.

Finally, one would expect to find genes encoding a hydroxylase, possibly a cytochrome P450-dependent enzyme plus an *O*-methyl transferase that are required for the formation of chondramides A and B from C and D, respectively. No candidate genes were found in the sequenced region except for *orf6* exhibiting similarity to cephalosporin hydroxylases. However, inactivation of this gene had no effect on chondramide biosynthesis (data not shown). Therefore, the formation of the methoxy group remains obscure. There are other examples from myxobacterial biosynthetic “gene clusters” where post-PKS modification enzymes are not found within the boundaries of the gene locus [51, 87].

Following *cmdF*, genes encoding phosphoenolpyruvate (PEP) synthase (*orf3*), a sugar diphosphoesterase (*orf4*), a hypothetical protein (*orf5*), a cephalosporin hydroxylase (*orf6*), and a cation transporting ATPase (*orf7*) are found. Upstream of *cmdA*, open-reading frames with translation products showing similarity to D-aminoacylases, hypothetical proteins, and another PEP synthase are found. Surprisingly, a second copy of this PEP synthase, exhibiting high similarity (57% identity at the protein level) is located at the 3' end of *CmdD* (Figures 2A and 2B). This finding leads to the speculation that the chondramide biosynthetic gene cluster could have evolved by horizontal gene transfer and integration between *orf2* and *cmdE* of the *C. crocatus* Cm c5 genome. PEP synthase is known to catalyze the phosphorylation of pyruvate to PEP via a phospho-histidine intermediate [88]. Although enzymes with similarity to PEP synthases are assumed to play a role in natural product biosynthesis in actinomycetes [89], inactivation of *orf2* and *orf3* showed no involvement of the PEP synthases in the biosynthesis of chondramides. Identical ratios of the various chondramides are produced in the respective mutants. A probable promoter for the chondramide gene cluster was identified in the region 51 bp upstream of the *orf2* stop codon. This region was unchanged by the inactivation of *orf2*.

## Significance

The highly cytotoxic chondramides and jaspamide are representative members of an important family of mixed PKS/NRPS derived natural product that have gained widespread use as tools to study the role of actin polymerization and depolymerization in various cellular functions. These compounds are also prime examples of strikingly similar natural products being

isolated from terrestrial microorganisms and marine invertebrate animals and fuel speculation as to the identity of the organism actually producing the marine natural product. Further adding to the interest in these compounds is the biochemistry leading to the rare  $\beta$ -tyrosine, or  $\alpha$ -methoxy- $\beta$ -tyrosine, residue and the unique 2-bromo- or 2-chlorotryptophans. Importantly, the cloned chondramide biosynthetic gene cluster can now be transferred to more easily manipulated host cells, which could increase production and facilitate analog development. These terrestrial genes may also provide useful information in the search for the marine natural product biosynthetic genes or serve as the starting point to create synthetic gene clusters for related compounds like jaspamide.

## Experimental Procedures

Standard methods for DNA isolation and manipulation were used as described by Kieser et al. [90] and Sambrook and Russell [91]. DNA fragments were isolated from agarose gels with the NucleoSpin Extract gel extraction kit (Macherey-Nagel, Düren, Germany). Southern analysis of genomic DNA was performed with the DIG DNA labeling and detection kit (Boehringer Mannheim, Germany). Hybridization was performed with a buffer containing 50% formamide at 42°C for homologous probes with stringent washes at 68°C. For heterologous probes, hybridization was performed at 37°C with stringent washes at 60°C. Other manipulations were performed according to the manufacturer's protocol. PCR was carried out with Taq DNA polymerase (Gibco BRL). Conditions for amplification using an Eppendorf Mastercycler gradient thermal cycler were as follows: denaturation, 30 s at 95°C; annealing, 30 s at 48°C–60°C; extension, 45 s at 72°C; 30 cycles and a final extension for 10 min at 72°C. PCR products were purified with the High Pure PCR Product Purification Kit (Boehringer Mannheim).

## Construction of the Cosmid Library

Chromosomal DNA of *Chondromyces crocatus* Cm c5 was partially digested with *Sau3AI*, dephosphorylated, and subsequently ligated into SuperCos 1 (Stratagene) pretreated with *XbaI*, dephosphorylated, and restricted with *BamHI*. Packaging of the ligation mixture with Gigapack III Gold (Stratagene) packaging extract and transducing the resulting phages into *E. coli* SURE (Stratagene) generated a genomic library consisting of 2304 clones.

## Screening of the Cosmid Library for the Chondramide Gene Cluster

All single colonies were transferred into 384-well microtiter plates, grown in LB medium overnight, and replicated twice. Glycerol (25%) was added to one copy of the library, and the plates were frozen at –80°C. For colony hybridization, the colonies of the second copy were transferred twice onto a 22.2 × 22.2 cm nylon membrane (Biodyne B, Pall) with a Qbot robot (Genetix) as previously described [32].

The membrane was incubated for 5 min on blotting paper prewetted with solutions I (0.5 M NaOH, 1 M Tris/HCl [pH 8.0]) and II (1.5 M NaCl, 1 M Tris/HCl [pH 8.0]), respectively. After drying for 15 min, the filters were UV-cross-linked with a Stratalinker (Stratagene). Bacterial debris was removed with tissue prewetted with 60°C prewarmed prehybridization solution. For the screening of the cosmid library, hybridization was performed with homologous and heterologous ketosynthase (KS) fragments as probes under low stringency conditions. The heterologous KS fragments were derived from three sources: *S. cellulosum* So ce90, *S. aurantiaca* Sg a15 [8], and from the *mtaB* gene, which is part of the myxothiazol biosynthetic cluster [33]. Homologous KS fragments approximately 700 bp in size were amplified from the genome of *C. crocatus* Cm c5 with the degenerate oligonucleotides KS1UP and KSD1 [8] designed to bind to conserved regions within KS domains. Additionally, the cosmid library was screened with homologous NRPS probes amplified from the genome of *C. crocatus* Cm c5 with degenerate primers RevA3 and

PSLGG designed to recognize the regions corresponding to the conserved A3 and A10 motifs within the NRPS adenylation (A) domains [34, 35].

A total of 42 cosmids that hybridized with both KS and NRPS probes were subjected to PCR analysis for the amplification of NRPS A domains (primers used were RevA3 and PSLGG). The resulting PCR products were gel purified and subcloned into pCR2.1TOPO vector (Invitrogen) and sequenced. Several identical NRPS sequences from different cosmids were found, which showed that the corresponding cosmids must overlap. The eight critical residues responsible for substrate recognition [36, 37] were extracted from the sequence enabling an *in silico* prediction of the substrate specificity of each cloned A domain fragment. Cosmids harbouring A domains that were predicted to activate alanine, tryptophan, or tyrosine were digested with *Bam*HI, and the restriction pattern was compared to identify similar cosmids. Finally, one representative of each cosmid group was end sequenced from the T3 and the T7 termini of the SuperCos vector. Oligonucleotide pairs based on the sequences obtained were designed and used to screen all other cosmids for the presence of overlapping sequences. The cosmid C:K13 carrying A domain sequences for the activation of alanine, N-methyltryptophan (as judged by the identification of an elongated PCR product with tryptophan specificity code also showing homology to N-methyltransferase domains) and tyrosine was found to overlap with a cosmid harboring only the NRPS A domain involved in the activation of tyrosine (B:O9).

Cosmids C:K13 and B:O9 were expected to carry the complete sequence of the chondramide biosynthetic gene cluster and were thus sequenced on both strands, by using a shotgun library with DNA fragments approximately 1.5–2.0 kb in length as described previously [33]. All sequence similarity searches were carried out on the amino acid level in the GenBank database with the BLAST program (release 2.0). Amino acid and nucleotide sequences were aligned with the Lasergene and Vector NTI software packages (DNASTAR and Invitrogen, respectively).

#### *Chondromyces crocatus* Cm c5 Conjugation

The lack of methodologies for genetic manipulation and transformation of *Chondromyces* species required that we develop methods for gene inactivation and DNA transfer into the chromosome of *C. crocatus* Cm c5. The transformation is based on biparental mating and conjugation with the methylation-deficient *E. coli* strain ET12567 harboring the pUB307 plasmid [38] and an insertion plasmid as donor strain. The conjugational transfer plasmids were constructed by first generating the insertion fragment by PCR. The resulting products were subcloned into the pCR2.1TOPO vector (Invitrogen), but because *C. crocatus* Cm c5 is not affected by kanamycin, the kanamycin resistance marker used with this vector cannot be used for the isolation of mutants. Therefore, the cloned fragment was excised with proper restriction enzymes and subcloned into the multiple cloning site of the conjugation plasmid pSUPHyg [39] carrying an *oriT* and the hygromycin resistance cassette, which can be used for *C. crocatus* Cm c5 selection. Mobilization of the plasmid into *C. crocatus* Cm c5 was done as follows: 50 ml of *C. crocatus* Cm c5 culture grown in Pol03 medium [9] for 5 days was centrifuged for 10 min at 5,000 rpm. The collected cell clumps were gently disaggregated and resuspended in 2 ml fresh Pol03 medium with a 5 ml glass homogenizer. The cells were centrifuged briefly at 3,000 rpm and gently resuspended in Pol03 medium to give a cell suspension of approximately  $10^{10}$  cells/ml. *E. coli* ET12567 cells, carrying pUB307 and the conjugational plasmid, were grown overnight in LB medium containing 100  $\mu$ g/ml hygromycin and 40  $\mu$ g/ml kanamycin. The culture was used for the inoculation of 50 ml LB medium and was grown at 37°C to OD<sub>600</sub> = 0.6–0.8. The cells were washed with MD1 medium at room temperature and resuspended to a final concentration of  $10^{10}$  cells/ml. The cell suspensions (100  $\mu$ l each) were mixed and incubated at 37°C in a thermomixer (Eppendorf) at 300 rpm for 3 hr. Next, the suspension was spotted onto Pol03-agar and incubated at 37°C for 40 hr. Subsequently, the cells were transferred into 1 ml of Pol03 medium by adding the medium to the agar plate and resuspending all cells by scraping the agar surface. Aliquots of 300  $\mu$ l were plated onto Pol03 agar containing tobramycin (80  $\mu$ g/ml) and hygromycin (100  $\mu$ g/ml) and incubated at 30°C. Mutant colonies of *C. crocatus* Cm c5 were observed after 5–7 days

of growth. The growth of the exconjugants had to be controlled regularly to prevent swarming, which can quickly prevent the possibility of picking single colonies (see Figures 1B and 1C). Single exconjugants were transferred into 5 ml of the Pol03 medium containing 100  $\mu$ g/ml hygromycin and incubated at 30°C for 7 days in a rotary shaker at 180 rpm. For chromosomal DNA isolation, the cell clumps were transferred into a 250 ml conical flask containing 50 ml of MD1 medium and incubated at 30°C with 100  $\mu$ g/ml hygromycin. For HPLC analysis of the secondary metabolite profile, cell clumps were used to inoculate Pol03 medium with 1% adsorber-Harz XAD 16 resin (Rohm & Haas, Frankfurt/Main, Germany) as described previously [9].

#### Inactivation of the Chondramide Biosynthetic Gene Cluster

An NRPS gene in the chondramide biosynthesis gene cluster was targeted for inactivation by insertional disruption with an internal fragment of an adenylation domain. A 1135 bp internal fragment of the A domain (A5) from the *cmdC* gene was amplified by PCR with the oligonucleotides RevA3: (5'-CCT CCG G[G]C C[G]A CCG G[G]C[AC] CGC C[G]C[A AGG-3') and PSLGG: (5'-GCC GCC [G]C[AG [G]C[CT] GAA GAA-3') and the cosmid B:O9 as template DNA. Conditions for amplification were as follows: denaturation, 30 s at 95°C; annealing, 30 s at 50°C; extension, 45 s at 72°C. The PCR fragment of the expected size was cloned into pCR2.1-TOPO and sequenced. The cloned fragment was excised with *Hind*III and *Eco*RV and cloned into pSUPHyg creating a conjugation plasmid designated pSBO9. The plasmid was electroporated into *E. coli* strain ET12567 containing pUB307, and the resulting clones were used for conjugation and transfer of pSBO9 into *C. crocatus* Cm c5 as described above. The mutant resulting after homologous recombination of pSBO9 into the genome was designated *C. crocatus* Mut20. It was grown in Pol03 medium containing hygromycin (100  $\mu$ g/ml) at 30°C for 7 days in a rotary shaker at 180 rpm with 1% adsorber-Harz (XAD) to analyze metabolite production as described previously [9]. The mutant strain was also grown in 50 ml MD1 medium for chromosomal DNA isolation. For verification of the plasmid insertion, the oligonucleotides pSUP-EV: (5'-GCATATAGCGCTAG CAGC-3') and RevA3 were used in PCR containing wild-type and mutant chromosomes. Furthermore, Southern blot analysis of the *Bam*HI digested chromosome of *C. crocatus* Cm c5 and two NRPS mutants was performed with a Dig-labeled internal fragment of the NRPS as hybridization probe.

#### Inactivation of the Halogenase Gene, *cmdE*

Inactivation of *cmdE*, the putative halogenase gene, was done by generating a 1138 bp internal fragment of the gene leading to a frame-shift mutation in the N-terminal sequence. By using genomic DNA of *C. crocatus* Cm c5 as template, PCR was carried out with oligonucleotides Halo-frame-up (5'-AGA TCC TTG TTC GTA GGT G-3') and Halo-mut-dn (5'-TGC GAC ATG TTG AAG ACG-3'). The PCR product was cloned into pCR2.1TOPO, the resulting plasmid was transformed into *E. coli*, and the product was verified by sequencing. Next, the fragment was subcloned into the *Eco*RV and *Bam*HI sites of pSUPHyg to create the insertion plasmid pSHAL. This plasmid was transferred by conjugation into *C. crocatus* Cm c5 leading to gene inactivation after homologous recombination. Mutants Cmc-Hal<sup>-</sup> were analyzed by PCR with the oligonucleotides Halo-frame-up and pSUP-EV as described above. Correct clones were further verified by Southern analysis (data not shown) and analyzed for chondramide production by HPLC-MS. Separation was carried out with an Agilent 1100 series system equipped with a photodiode array detector and coupled to a Bruker HCTplus mass spectrometer operated in positive ionization mode at a scan range from  $m/z$  = 100–1100. A 125 × 2mm Nucleodur C18/3  $\mu$ m RP column (Macherey & Nagel) was used for separation with a solvent system consisting of H<sub>2</sub>O (A) and acetonitrile (B), each containing 0.1% formic acid. The following gradient was applied: 0–2 min 5% B, 2–32 min linear from 5% B to 95% B, 32–35 min isocratic at 95% B. Chondramides were identified by comparison to the retention times and the MS data of authentic standards (chondramide A:  $r_t$  = 15.9 min, [M+H]<sup>+</sup> = 647; chondramide C:  $r_t$  = 16.7 min, [M+H]<sup>+</sup> = 617; chondramide B:  $r_t$  = 16.9 min, [M+H]<sup>+</sup> = 681; chondramide D:  $r_t$  = 18.0 min, [M+H]<sup>+</sup> = 641).



### Transcriptional Analysis of the TAM Gene in the *cmdE* Mutant Cmc-Hal<sup>-</sup>

*C. crocatus* Cmc-Hal<sup>-</sup> was grown in Pol03 with 100 µg/ml hygromycin for 5 days at 30°C. Bacterial cells were collected by centrifugation at 5000 rpm. Transcriptional analysis of *cmdE* expression in wild-type and mutant cells was performed by Northern blot analysis of the bacterial total RNA, which was isolated with the FastRNA Kit, BLUE (BIO 101, Germany) according to the manufacturer's protocol. A 1060 bp internal fragment of *cmdE* was generated by PCR with TAM-up (5'-CTC CAA CCT GTC CAT CTA C-3') and TAM-dn (5'-GAT GTT CAG GTA GTC GCA G-3'), labeled with digoxigenin by using DIG High Prime kit (Roche) and used as a probe in the Northern blot (hybridization was performed at 42°C).

### Inactivation of Orf2, Orf3, and Orf6

Inactivation of orf2 located upstream the gene cluster and encoding a putative phosphoenolpyruvate synthase, orf3 (the second putative phosphoenolpyruvate synthase), and orf6 (the putative cephalosporin hydroxylase) was performed analogously with the inactivation plasmids pSR4, pSR5, and pSR6, respectively. These plasmids were constructed by cloning 921 bp, 649 bp, and 604 bp (with a frame-shift mutation in the 5' sequence) PCR products generated with the oligonucleotides PEP1-up (5'-GGTTACGAGCACTACG G-3') and PEP1-dn (TGGTAGGTGATCTTGCGAG -3'), PEP3-frame-up (5'-ATGCGTGCGCATCCTCTGGCTG-3') and PEP3-dn (5'-GGTTC ATGTTCTGCTTCTC-3'), and Ceph-up (5'-GCC AGA TGA CCA CCT CTA C-3') and Ceph-dn (5'-GACGTAGTAGTCGCCCTC-3'), respectively. The plasmids were transferred by conjugation into *C. crocatus* Cm c5 leading to gene inactivation after homologous recombination, which was verified by Southern blot and PCR analysis (data not shown). The resulting mutants Cmc-orf2, Cmc-orf3, and Cmc-orf6 were analyzed by HPLC-MS for chondramide production.

### Incorporation of Fluorotryptophan into Chondramides

To test the incorporation of nonchlorinated tryptophan into the structure of chondramide, 5-fluorotryptophan (Fluka) was added to a 100 ml culture of the *C. crocatus* Cm c5 in equal portions (final concentration of 1 mM) at 24, 48, and 72 hr after the inoculation. XAD resin (1% V/V) was added, the culture was grown for 7 days at 30°C, and cells and resin were harvested and extracted with methanol. The solvent was removed, and the residue was dissolved in 500 µl of methanol, and 10 µl of this concentrated extract was analyzed by HPLC-MS/MS.

### Amplification and Cloning of the Chondramide A<sub>7</sub> Domain

The pGEX-6P-1 (Amersham Biosciences) overexpression system was used to express a 1709 bp PCR product corresponding to the adenylation domain from module 7 (A<sub>7</sub>). PCR with chromosomal DNA of *C. crocatus* Cm c5 was carried out with PFU polymerase (Stratagene) by using oligonucleotides Tyr-Ad-up (5'-GGAATT-CATGGACGAACAGAGGAAG-3'; introduced *EcoRI* site is in bold) and Tyr-Ad-dn (5'-GAGCTTGAAGAATCGTC-3'). The resulting PCR product was purified and cloned into pCR2.1TOPO, creating pTOPO-Ad7. After checking the sequence fidelity, the insert was excised from the vector and subcloned into the *EcoRI* site of the expression vector pGEX-6P-1 creating pGEX-Ad-7.

### Overexpression and Purification of the Adenylation Domain A<sub>7</sub>

Plasmid pGEX-Ad-7 was transformed into *E. coli* BL21, and cells were grown in LB medium supplemented with 100 µg/ml ampicillin at 30°C. Expression was induced with 0.2 mM IPTG (isopropyl-β-D-thiogalactopyranoside) at an OD<sub>600nm</sub> = 0.6–0.8, and the cells were allowed to grow for an additional 2 hr before harvest. The A<sub>7</sub> protein was expressed as an N-terminal GST-fusion protein. Purification of the protein was carried out by glutathione affinity chromatography and on-column GST-fusion protein cleavage with PreScission Protease at 4°C according to the manufacturer's recommendations.

### ATP-Pi Exchange Reactions

Assays were performed following described methods [40] and were carried out at 25°C in 100 µl total volume containing 50 mM Tris (pH 8.0), 10 mM MgCl<sub>2</sub>, 100 mM NaCl, 1 mM EDTA, 1 mM DTT, 2 mM dATP, 150 nM A<sub>7</sub>, 1 mM [<sup>32</sup>P]-pyrophosphate (0.5 µCi), and 2 mM

of either L-tyrosine, (R,S)-β-tyrosine (Johnson Pump, UK), L-tryptophan, L-phenylalanine, or L-methionine as possible substrates. The reactions were allowed to proceed for 15 min at 25°C and then quenched by addition of a charcoal-tetrasodium pyrophosphate-perchloric acid mixture (1.6% [w/v] activated charcoal, 4.46% [w/v] tetrasodium pyrophosphate, 3.5% perchloric acid in water). The charcoal was pelleted by centrifugation, washed twice with the quenching mixture (without charcoal), and then resuspended in 0.5 ml water and submitted for liquid scintillation counting. The reactions were typically performed in triplicate.

### Acknowledgments

The authors would like to thank Y. Elnakady for fluorescence microscopic images. Research in R.M.'s laboratory was funded by the Bundesministerium für Bildung und Forschung and the Deutsche Forschungsgemeinschaft.

Received: January 3, 2006

Revised: February 16, 2006

Accepted: March 20, 2006

Published: June 23, 2006

### References

1. Bode, H.B., and Müller, R. (2005). The impact of bacterial genomics on natural product research. *Angew. Chem. Int. Ed. Engl.* 44, 6828–6846.
2. Weissman, K.J., and Leadlay, P.F. (2005). Combinatorial biosynthesis of reduced polyketides. *Nat. Rev. Microbiol.* 3, 925–936.
3. Newman, D., Cragg, G., and Snader, K. (2003). Natural products as sources of new drugs over the period 1981–2002. *J. Nat. Prod.* 66, 1022–1037.
4. Reichenbach, H., and Höfle, G. (1999). Myxobacteria as producers of secondary metabolites. In *Drug Discovery from Nature*, S. Grabley and R. Thiericke, eds. (Berlin: Springer), pp. 149–179.
5. Reichenbach, H. (2001). Myxobacteria, producers of novel bioactive substances. *J. Ind. Microbiol. Biotechnol.* 27, 149–156.
6. Gerth, K., Pradella, S., Perlova, O., Beyer, S., and Müller, R. (2003). Myxobacteria: proficient producers of novel natural products with various biological activities—past and future biotechnological aspects with the focus on the genus *Sorangium*. *J. Biotechnol.* 106, 233–253.
7. Silakowski, B., Kunze, B., and Müller, R. (2001). Multiple hybrid polyketide synthase/non-ribosomal peptide synthetase gene clusters in the myxobacterium *Stigmatella aurantiaca*. *Gene* 275, 233–240.
8. Beyer, S., Kunze, B., Silakowski, B., and Müller, R. (1999). Metabolic diversity in myxobacteria: identification of the myxalamid and the stigmatellin biosynthetic gene cluster of *Stigmatella aurantiaca* Sg a15 and a combined polyketide-(poly)peptide gene cluster from the epothilone producing strain *Sorangium cellulosum* So ce90. *Biochim. Biophys. Acta* 1445, 185–195.
9. Kunze, B., Jansen, R., Sasse, F., Höfle, G., and Reichenbach, H. (1995). Chondramides A approximately D, new antifungal and cytostatic depsipeptides from *Chondromyces crocatus* (myxobacteria). Production, physico-chemical and biological properties. *J. Antibiot. (Tokyo)* 48, 1262–1266.
10. Jansen, R., Kunze, B., Reichenbach, H., and Höfle, G. (1996). Chondramides A-D, new cytostatic and antifungal cyclodepsipeptides from *Chondromyces crocatus* (myxobacteria): isolation and structure elucidation. *Liebigs Ann.* 2, 285–290.
11. Kunze, B., Jansen, R., Höfle, G., and Reichenbach, H. (2004). Ajudazols, new inhibitors of the mitochondrial electron transport from *Chondromyces crocatus*. Production, antimicrobial activity and mechanism of action. *J. Antibiot. (Tokyo)* 57, 151–155.
12. Jansen, R., Kunze, B., Reichenbach, H., and Höfle, G. (2003). Chondrochloren A and B, new beta-amino styrenes from *Chondromyces crocatus* (myxobacteria). *Eur. J. Org. Chem.* 2003, 2684–2689.
13. Sasse, F., Kunze, B., Gronewold, T.M., and Reichenbach, H. (1998). The chondramides: cytostatic agents from myxobacteria



- acting on the actin cytoskeleton. *J. Natl. Cancer Inst.* **90**, 1559–1563.
14. Kunze, B., Jansen, R., Höfle, G., and Reichenbach, H. (1994). Crocacin, a new electron transport inhibitor from *Chondromyces crocatus* (myxobacteria). Production, isolation, physicochemical and biological properties. *J. Antibiot. (Tokyo)* **47**, 881–886.
15. Jansen, R., Washausen, P., Kunze, B., Reichenbach, H., and Höfle, G. (1999). Antibiotics from gliding bacteria, LXXXIII. The crocacins, novel antifungal and cytotoxic antibiotics from *Chondromyces crocatus* and *Chondromyces pediculatus* (Myxobacteria): isolation and structure elucidation. *Eur. J. Org. Chem.* **1999**, 1085–1089.
16. Zabriskie, T.M., Klocke, J.A., Ireland, C.M., Marcus, A.H., Molinski, T.F., Faulkner, D.J., Xu, C., and Clardy, J. (1986). Jaspamide, a modified peptide from a *Jaspis* sponge, with insecticidal and antifungal activity. *J. Am. Chem. Soc.* **108**, 3123–3124.
17. Crews, P., Manes, L.V., and Boehler, M. (1986). Jaspakinolide, a cyclodepsipeptide from the marine sponge *Jaspis* sp. *Tetrahedron Lett.* **27**, 2797–2800.
18. Braekman, J.C., Daloz, D., and Moussiaux, B. (1987). Jaspamide from the marine sponge *Jaspis johnstoni*. *J. Nat. Prod.* **50**, 994–995.
19. Coleman, J.E., de Silva, E.D., Kong, F., and Andersen, R.J. (1995). Cytotoxic peptides from the marine sponge *Cymbastela* sp. *Tetrahedron* **51**, 10653–10662.
20. Chan, W.R., Tinto, W.F., Manchand, P.S., and Todaro, L.J. (1987). Stereostructures of geodiamolides A and B, novel cyclodepsipeptides from the marine sponge *Geodia* sp. *J. Org. Chem.* **52**, 3091–3093.
21. de Silva, E.D., Andersen, R.J., and Allen, T.M. (1990). Geodiamolides C to F, new cytotoxic cyclodepsipeptides from the marine sponge *Pseudaxynysa* sp. *Tetrahedron Lett.* **31**, 489–492.
22. Talpir, R., Benayahu, Y., Kashman, Y., Pannell, L., and Schleyer, M. (1994). Hemiasterlin and geodiamolide TA; two new cytotoxic peptides from the marine sponge *Hemiasterella minor* (Kirkpatrick). *Tetrahedron Lett.* **35**, 4453–4456.
23. D'Auria, M.V., Gomez Paloma, L., Minale, L., Zampella, A., Debitus, C., and Perez, J. (1995). Neosiphoniamolide A, a novel cyclodepsipeptide, with antifungal activity from the marine sponge *Neosiphonia superstes*. *J. Nat. Prod.* **58**, 121–123.
24. Wolff, A., Technau, A., and Brandner, G. (1997). Epothilone A induces apoptosis in neuroblastoma cells with multiple mechanisms of drug resistance. *Int. J. Oncol.* **11**, 123–126.
25. Gronewold, T.M., Sasse, F., Lunsdorf, H., and Reichenbach, H. (1999). Effects of rhizopodin and latrunculin B on the morphology and on the actin cytoskeleton of mammalian cells. *Cell Tissue Res.* **295**, 121–129.
26. Low, I., Dancker, P., and Wieland, T. (1975). Stabilization of F-actin by phalloidin. Reversal of the destabilizing effect of cytochalasin B. *FEBS Lett.* **54**, 263–265.
27. Holzinger, A., and Lutz-Meindl, U. (2001). Chondramides, novel cyclodepsipeptides from myxobacteria, influence cell development and induce actin filament polymerization in the green alga *Micrasterias*. *Cell Motil. Cytoskeleton* **48**, 87–95.
28. Tang, L., Shah, S., Chung, L., Carney, J., Katz, L., Khosla, C., and Julien, B. (2000). Cloning and heterologous expression of the epothilone gene cluster. *Science* **287**, 640–642.
29. Walsh, C. (2003). *Antibiotics: Actions, Origins, Resistance* (Washington, DC: ASM Press).
30. Kwon, H.J., Smith, W.C., Xiang, L., and Shen, B. (2001). Cloning and heterologous expression of the macrotretrolide biosynthetic gene cluster revealed a novel polyketide synthase that lacks an acyl carrier protein. *J. Am. Chem. Soc.* **123**, 3385–3386.
31. Wenzel, S.C., Gross, F., Zhang, Y., Fu, J., Stewart, F.A., and Müller, R. (2005). Heterologous expression of a myxobacterial natural products assembly line in pseudomonads via red/ET recombineering. *Chem. Biol.* **12**, 349–356.
32. Dunham, I., Dewar, K., Kim, U.-J., and Ross, M.T. (1997). Bacterial cloning systems. In *Genome Analysis. A Laboratory Manual. Cloning Systems, Volume 3*, B. Birren, E.D. Green, S. Klapholz, R.M. Myers, and J. Roskams, eds. (New York: Cold Spring Harbor Laboratory Press), pp. 1–86.
33. Silakowski, B., Schairer, H.U., Ehret, H., Kunze, B., Weinig, S., Nordsiek, G., Brandt, P., Blöcker, H., Höfle, G., Beyer, S., et al. (1999). New lessons for combinatorial biosynthesis from myxobacteria: the myxothiazol biosynthetic gene cluster of *Stigmatella aurantiaca* DW4/3-1. *J. Biol. Chem.* **274**, 37391–37399.
34. Marahiel, M.A., Stachelhaus, T., and Mootz, H.D. (1997). Modular peptide synthetases involved in nonribosomal peptide synthesis. *Chem. Rev.* **97**, 2651–2674.
35. Konz, D., and Marahiel, M.A. (1999). How do peptide synthetases generate structural diversity? *Chem. Biol.* **6**, R39–R48.
36. Stachelhaus, T., Mootz, H.D., and Marahiel, M.A. (1999). The specificity-conferring code of adenylation domains in nonribosomal peptide synthetases. *Chem. Biol.* **6**, 493–505.
37. Challis, G.L., Ravel, J., and Townsend, C.A. (2000). Predictive, structure-based model of amino acid recognition by nonribosomal peptide synthetase adenylation domains. *Chem. Biol.* **7**, 211–224.
38. Kopp, M., Irschik, H., Gross, F., Perlova, O., Sandmann, A., Gerth, K., and Müller, R. (2004). Critical variations of conjugational DNA transfer into secondary metabolite multiproducing *Sorangium cellulosum* strains So ce12 and So ce56: development of a mariner-based transposon mutagenesis system. *J. Biotechnol.* **107**, 29–40.
39. Knauber, J. (2004). Untersuchungen zum Genetischen Potential der Sekundärstoffbildung von *Sorangium cellulosum* So ce90 und Identifizierung des Spirangienbiosynthesegenclusters. PhD thesis, Technische Universität Carolo-Wilhelmina, Braunschweig.
40. Stachelhaus, T., and Marahiel, M.A. (1995). Modular structure of peptide synthetases revealed by dissection of the multifunctional enzyme GrsA. *J. Biol. Chem.* **270**, 6163–6169.
41. Pradella, S., Hans, A., Sproer, C., Reichenbach, H., Gerth, K., and Beyer, S. (2002). Characterisation, genome size and genetic manipulation of the myxobacterium *Sorangium cellulosum* So ce56. *Arch. Microbiol.* **178**, 484–492.
42. de Crecy-Lagard, V., Blanc, V., Gil, P., Naudin, L., Lorenzon, S., Famechon, A., Bamas-Jacques, N., Crouzet, J., and Thibaut, D. (1997). Pristinamycin I biosynthesis in *Streptomyces pristinaespiralis*: molecular characterization of the first two structural peptide synthetase genes. *J. Bacteriol.* **179**, 705–713.
43. Shimkets, L. (1993). The myxobacterial genome. In *Myxobacteria II*, M. Dworkin and D. Kaiser, eds. (Washington, DC: American Society for Microbiology), pp. 85–108.
44. Ishikawa, J., and Hotta, K. (1999). FramePlot: a new implementation of the frame analysis for predicting protein-coding regions in bacterial DNA with a high G + C content. *FEMS Microbiol. Lett.* **174**, 251–253.
45. Jacobi, C.A., Reichenbach, H., Tindall, B.J., and Stackebrandt, E. (1996). "Candidatus comitans," a bacterium living in coculture with *Chondromyces crocatus* (myxobacteria). *Int. J. Syst. Bacteriol.* **46**, 119–122.
46. Du, L., Sanchez, C., Chen, M.T., Edwards, D., and Shen, B. (2000). The biosynthetic gene cluster for the antitumor drug bleomycin from *Streptomyces verticillus* ATCC15003 supporting functional interactions between nonribosomal peptide synthetases and a polyketide synthase. *Chem. Biol.* **7**, 623–642.
47. Yadav, G., Gokhale, R.S., and Mohanty, D. (2003). SEARCHPKS: a program for detection and analysis of polyketide synthase domains. *Nucleic Acids Res.* **31**, 3654–3658.
48. Yadav, G., Gokhale, R.S., and Mohanty, D. (2003). Computational approach for prediction of domain organization and substrate specificity of modular polyketide synthases. *J. Mol. Biol.* **328**, 335–363.
49. Gaitatzis, N., Silakowski, B., Kunze, B., Nordsiek, G., Blöcker, H., Höfle, G., and Müller, R. (2002). The biosynthesis of the aromatic myxobacterial electron transport inhibitor stigmatellin is directed by a novel type of modular polyketide synthase. *J. Biol. Chem.* **277**, 13082–13090.
50. Wenzel, S.C., Kunze, B., Höfle, G., Silakowski, B., Scharfe, M., Blöcker, H., and Müller, R. (2005). Structure and biosynthesis of myxochromides S1–3 in *Stigmatella aurantiaca*: evidence for an iterative bacterial type I polyketide synthase and for module skipping in nonribosomal peptide biosynthesis. *ChemBioChem* **6**, 375–385.

51. Kopp, M., Irschik, H., Pradella, S., and Müller, R. (2005). Production of the tubulin destabilizer disorazol in *Sorangium cellulosum*: biosynthetic machinery and regulatory genes. *ChemBioChem* 6, 1277–1286.
52. Perlova, O., Gerth, K., Hans, A., Kaiser, O., and Müller, R. (2005). Identification and analysis of the chivosazol biosynthetic gene cluster from the myxobacterial model strain *Sorangium cellulosum* So ce56. *J. Biotechnol.* 121, 174–191.
53. Wenzel, S.C., and Müller, R. (2005). Formation of novel secondary metabolites by bacterial multimodular assembly lines: deviations from text book biosynthetic logic. *Curr. Opin. Chem. Biol.* 9, 447–458.
54. Silakowski, B., Nordsiek, G., Kunze, B., Blöcker, H., and Müller, R. (2001). Novel features in a combined polyketide synthase/non-ribosomal peptide synthetase: the myxalamid biosynthetic gene cluster of the myxobacterium *Stigmatella aurantiaca* Sga15. *Chem. Biol.* 8, 59–69.
55. Ligon, J., Hill, S., Beck, J., Zirkle, R., Monar, I., Zawodny, J., Money, S., and Schupp, T. (2002). Characterization of the biosynthetic gene cluster for the antifungal polyketide soraphen A from *Sorangium cellulosum* So ce26. *Gene* 285, 257–267.
56. Weinig, S., Hecht, H.J., Mahmud, T., and Müller, R. (2003). Melithiazol biosynthesis: further insights into myxobacterial PKS/NRPS systems and evidence for a new subclass of methyl transferases. *Chem. Biol.* 10, 939–952.
57. Wilkinson, C.J., Frost, E.J., Staunton, J., and Leadlay, P.F. (2001). Chain initiation on the soraphen-producing modular polyketide synthase from *Sorangium cellulosum*. *Chem. Biol.* 8, 1197–1208.
58. Haydock, S., Aparicio, J.F., Molnar, I., Schwecke, T., König, A., Marsden, A.F.A., Galloway, I.S., Staunton, J., and Leadley, P.F. (1995). Divergent structural motifs correlated with the substrate specificity of (methyl)malonyl-CoA:acylcarrier protein transacylase domains in the modular polyketide synthases. *FEBS Lett.* 374, 246–248.
59. Ikeda, H., Nonomiya, T., Usami, M., Ohta, T., and Omura, S. (1999). Organization of the biosynthetic gene cluster for the polyketide anthelmintic macrolide avermectin in *Streptomyces avermitilis*. *Proc. Natl. Acad. Sci. USA* 96, 9509–9514.
60. Donadio, S., and Katz, L. (1992). Organization of the enzymatic domains in the multifunctional polyketide synthase involved in erythromycin formation in *Saccharopolyspora erythraea*. *Gene* 111, 51–60.
61. Scrutton, N.S., Berry, A., and Perham, R.N. (1990). Redesign of the coenzyme specificity of a dehydrogenase by protein engineering. *Nature* 343, 38–43.
62. Caffrey, P. (2003). Conserved amino acid residues correlating with ketoreductase stereospecificity in modular polyketide synthases. *ChemBioChem* 4, 654–657.
63. Conti, E., Stachelhaus, T., Marahiel, M.A., and Brick, P. (1997). Structural basis for the activation of phenylalanine in the non-ribosomal biosynthesis of gramicidin S. *EMBO J.* 16, 4174–4183.
64. Rouhiainen, L., Vakkilainen, T., Siemer, B.L., Buikema, W., Haselkorn, R., and Sivonen, K. (2004). Genes coding for hepatotoxic heptapeptides (microcystins) in the cyanobacterium *Anabaena* strain 90. *Appl. Environ. Microbiol.* 70, 686–692.
65. Edwards, D.J., Marquez, B.L., Nogle, L.M., McPhail, K., Goeger, D.E., Roberts, M.A., and Gerwick, W.H. (2004). Structure and biosynthesis of the jamaicamides, new mixed polyketide-peptide neurotoxins from the marine cyanobacterium *Lyngbya majuscula*. *Chem. Biol.* 11, 817–833.
66. Mootz, H.D., and Marahiel, M.A. (1997). The tyrocidine biosynthesis operon of *Bacillus brevis*: complete nucleotide sequence and biochemical characterization of functional internal adenylation domains. *J. Bacteriol.* 179, 6843–6850.
67. Kagan, R.M., and Clarke, S. (1994). Widespread occurrence of three sequence motifs in diverse S-adenosylmethionine-dependent methyltransferases suggest a common structure for these enzymes. *Arch. Biochem. Biophys.* 310, 417–427.
68. Linne, U., Doekel, S., and Marahiel, M.A. (2001). Portability of epimerization domain and role of peptidyl carrier protein on epimerization activity in nonribosomal peptide synthetases. *Biochemistry* 40, 15824–15834.
69. Stachelhaus, T., and Walsh, C.T. (2000). Mutational analysis of the epimerization domain in the initiation module PheATE of gramicidin S synthetase. *Biochemistry* 39, 5775–5787.
70. Stein, T., Kluge, B., Vater, J., Franke, P., Otto, A., and Wittmann-Liebold, B. (1995). Gramicidin S synthetase 1 (phenylalanine racemase), a prototype of amino acid racemases containing the cofactor 4'-phosphopantetheine. *Biochemistry* 34, 4633–4642.
71. Belshaw, P., Walsh, C., and Stachelhaus, T. (1999). Aminoacyl-CoAs as probes of condensation domain selectivity in nonribosomal peptide synthesis. *Science* 284, 486–489.
72. Clugston, S.L., Sieber, S.A., Marahiel, M.A., and Walsh, C.T. (2003). Chirality of peptide bond-forming condensation domains in nonribosomal peptide synthetases: the C-5 domain of tyrocidine synthetase is a C-D(L) catalyst. *Biochemistry* 42, 12095–12104.
73. De Crecy-Lagard, V., Marliere, P., and Saurin, W. (1995). Multienzyme nonribosomal peptide biosynthesis: identification of the functional domains catalysing peptide elongation and epimerisation. *C. R. Acad. Sci. III* 318, 927–936.
74. Rouhiainen, L., Paulin, L., Suomalainen, S., Hyytiäinen, H., Buikema, W., Haselkorn, R., and Sivonen, K. (2000). Genes encoding synthetases of cyclic depsipeptides, anabaenopeptilides, in *Anabaena* strain 90. *Mol. Microbiol.* 37, 156–167.
75. Hoffmann, D., Hevel, J.M., Moore, R.E., and Moore, B.S. (2003). Sequence analysis and biochemical characterization of the nos-topeptolide A biosynthetic gene cluster from *Nostoc* sp. GSV224. *Gene* 311, 171–180.
76. Frey, P.A. (2001). Radical mechanisms of enzymatic catalysis. *Annu. Rev. Biochem.* 70, 121–148.
77. Walker, K.D., Klettke, K., Akiyama, T., and Croteau, R. (2004). Cloning, heterologous expression, and characterization of a phenylalanine aminomutase involved in Taxol biosynthesis. *J. Biol. Chem.* 279, 53947–53954.
78. Christenson, S.D., Wu, W., Spies, M.A., Shen, B., and Toney, M.D. (2003). Kinetic analysis of the 4-methylideneimidazole-5-one-containing tyrosine aminomutase in enediyne antitumor antibiotic C-1027 biosynthesis. *Biochemistry* 42, 12708–12718.
79. Christenson, S.D., Liu, W., Toney, M.D., and Shen, B. (2003). A novel 4-methylideneimidazole-5-one-containing tyrosine aminomutase in enediyne antitumor antibiotic C-1027 biosynthesis. *J. Am. Chem. Soc.* 125, 6062–6063.
80. Van Lanen, S.G., Dorrestein, P.C., Christenson, S.D., Liu, W., Ju, J., Kelleher, N.L., and Shen, B. (2005). Biosynthesis of the beta-amino acid moiety of the enediyne antitumor antibiotic C-1027 featuring beta-amino acyl-S-carrier protein intermediates. *J. Am. Chem. Soc.* 127, 11594–11595.
81. Luo, L., Burkart, M.D., Stachelhaus, T., and Walsh, C.T. (2001). Substrate recognition and selection by the initiation module PheATE of gramicidin S synthetase. *J. Am. Chem. Soc.* 123, 11208–11218.
82. Trauger, J.W., Kohli, R.M., and Walsh, C.T. (2001). Cyclization of backbone-substituted peptides catalyzed by the thioesterase domain from the tyrocidine nonribosomal peptide synthetase. *Biochemistry* 40, 7092–7098.
83. Staunton, J., and Wilkinson, B. (2001). Combinatorial biosynthesis of polyketides and nonribosomal peptides. *Curr. Opin. Chem. Biol.* 5, 159–164.
84. Dong, C., Flecks, S., Unversucht, S., Haupt, C., van Pee, K.H., and Naismith, J.H. (2005). Tryptophan 7-halogenase (PrnA) structure suggests a mechanism for regioselective chlorination. *Science* 309, 2216–2219.
85. Zehner, S., Kotsch, A., Bister, B., Sussmuth, R.D., Mendez, C., Salas, J.A., and van Pee, K.H. (2005). A regioselective tryptophan 5-halogenase is involved in pyrroindomycin biosynthesis in *Streptomyces rugosporus* LL-42D005. *Chem. Biol.* 12, 445–452.
86. Yeh, E., Garneau, S., and Walsh, C.T. (2005). Robust in vitro activity of RebF and RebH, a two-component reductase/halogenase, generating 7-chlorotryptophan during rebeccamycin biosynthesis. *Proc. Natl. Acad. Sci. USA* 102, 3960–3965.
87. Sandmann, A., Sasse, F., and Müller, R. (2004). Identification and analysis of the core biosynthetic machinery of tubulysin, a potent

- cytotoxin with potential anticancer activity. *Chem. Biol.* **11**, 1071–1079.
88. Niersbach, M., Kreuzaler, F., Geerse, R.H., Postma, P.W., and Hirsch, H.J. (1992). Cloning and nucleotide sequence of the *Escherichia coli* K-12 *ppsA* gene, encoding PEP synthase. *Mol. Gen. Genet.* **231**, 332–336.
  89. Cerdeno, A.M., Bibb, M.J., and Challis, G.L. (2001). Analysis of the prodiginine biosynthesis gene cluster of *Streptomyces coelicolor* A3(2): new mechanisms for chain initiation and termination in modular multienzymes. *Chem. Biol.* **8**, 817–829.
  90. Kieser, T., Bibb, M., Buttner, M.J., Chater, K.F., and Hopwood, D.A. (2000). *Practical Streptomyces Genetics* (Norwich, England: The John Innes Foundation).
  91. Sambrook, J., and Russell, D.W. (2001). *Molecular Cloning: A Laboratory Manual* (Cold Spring Harbor, NY: Cold Spring Harbor Laboratory Press).
  92. Serre, L., Verbree, E., Dauter, Z., Stuitje, A.R., and Derewenda, Z.S. (1995). The *Escherichia coli* malonyl-coa:acyl carrier protein transacylase at 1.5-angstroms resolution: crystal structure of a fatty acid synthase component. *J. Biol. Chem.* **270**, 12961–12964.

#### Accession Number

The DNA sequence reported in this paper has been entered into the EMBO database under the accession number [AM179409](#).